

## Early afterglow from a reverse shock as a tracer of the prompt gamma-ray light curve<sup>(\*)</sup>

E. NAKAR<sup>(1)</sup> and T. PIRAN<sup>(1)</sup>(<sup>2</sup>)

<sup>(1)</sup> *Theoretical astrophysics, Caltech - Pasadena, CA 91125, USA*

<sup>(2)</sup> *Racah Institute for Physics, The Hebrew University - Jerusalem 91904, Israel*

(ricevuto il 23 Maggio 2005; pubblicato online il 22 Settembre 2005)

**Summary.** — We discuss the optical and radio early afterglow emission of the reverse shock that crosses a baryonic ejecta as it interacts with the external interstellar medium (ISM). We show that the peak of the optical flash divided the reverse shock light curve into two distinctive phases. The emission after the peak depends weakly on the initial conditions of the ejecta and therefore it can be used as an identifiable signature of a reverse shock emission. On the other hand, the emission before the optical peak is highly sensitive to the initial conditions and therefore can be used to investigate the initial hydrodynamic profile of the ejecta. In particular, if the prompt  $\gamma$ -ray emission results from internal shocks, the early reverse shock emission should resemble a smoothed version of the prompt  $\gamma$ -ray light curve.

PACS 98.70.Rz –  $\gamma$ -ray sources;  $\gamma$ -ray bursts.

PACS 96.50.Fm – Shock waves.

PACS 95.30.Lz – Hydrodynamics.

PACS 01.30.Cc – Conference proceedings.

### 1. – Introduction

According to the internal-external shocks model the prompt gamma-ray burst (GRB) is produced by internal shocks within a relativistic flow while the afterglow is produced by external shocks between this flow and the surrounding matter. The early afterglow appears during the transition from the prompt  $\gamma$ -ray emission to the afterglow. During this transition the relativistic flow, ejected by the source, interacts directly with the circum burst medium. This interaction can be used to pin down the nature of the relativistic flow (baryonic or Poynting flux). In a baryonic flow the reverse shock (RS) that propagates into the ejecta produces both optical and radio emission. A Poynting flux flow is expected to produce only the higher energy forward shock emission. While other sources of early optical and radio emission may exist also in Poynting Flux, the RS emission has a very robust optical and radio observable signatures that are very unlikely to be imitated by other phenomena [1].

---

<sup>(\*)</sup> Paper presented at the “4th Workshop on Gamma-Ray Burst in the Afterglow Era”, Rome, October 18-22, 2004.

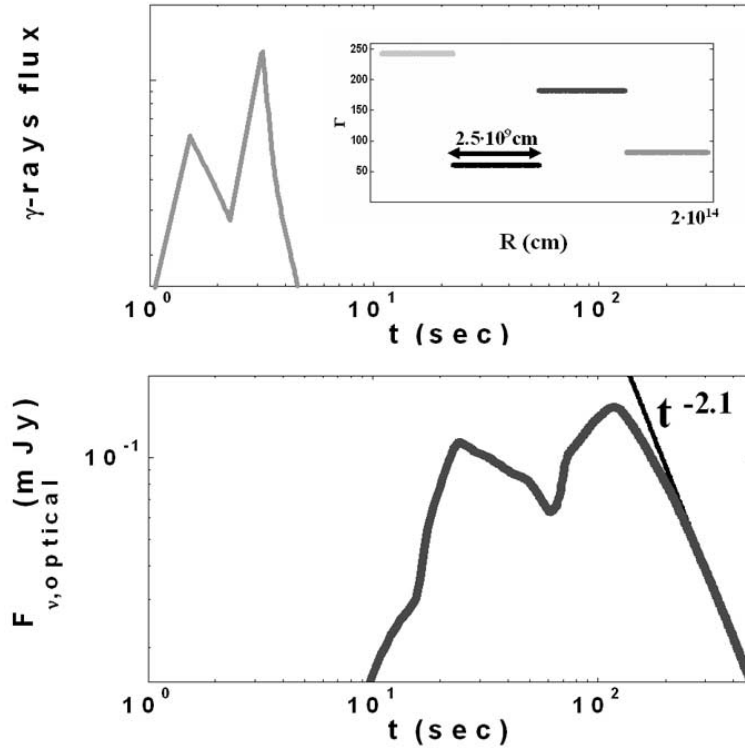


Fig. 1. – *Top*: An illustration of the prompt  $\gamma$ -ray emission (the flux is in arbitrary units) resulting from the collisions of four shells. The initial Lorentz factor and width of these four shells is depicted in the inset. *Bottom*: The optical light curve of the reverse shock as simulated numerically. The initial hydrodynamic profile of the simulation appears in the top panel inset. The total energy (isotropic equivalent) of the ejecta is  $8 \cdot 10^{51}$  erg and the external density is a constant  $10 \text{ cm}^{-3}$ . The energy equipartition parameters of the electrons and the magnetic field  $\epsilon_e = 0.5$  and  $\epsilon_B = 0.01$ , respectively. The electrons spectral index is  $p = 2.5$  and the burst is at a redshift  $z = 1$ . Note that the time axis is logarithmic.

In GRBs the reverse shock is mildly relativistic [2]. This implies that during one crossing the shock dissipates almost all the bulk motion energy of the outflow to internal energy. After a single crossing of the outflow a rarefaction wave is reflected and only the forward shock remains, forming the shocked external medium into a Blandford-McKee self-similar solution. The original ejecta expands and cools at the tail of the shocked external medium. The reverse shock emission can be divided into two distinctive phases, the RS crossing phase and the expanding-cooling phase. Observationally, the two are separated by the peak of the optical flash. The evolution before the time of the optical peak,  $t_0$ , is highly sensitive to the initial profile of the ejecta, namely to the density and the Lorentz factor of the ejecta at the beginning of the RS crossing. Thus the light curve before and at  $t_0$  can be used as a diagnostic tool of these properties. On the other hand, the RS that crosses the shell erases, to a large extent, the initial shell profile. Moreover, the evolution during the expanding and cooling phase depends only weakly on this profile [3]. Therefore, the behavior after  $t_0$  depends weakly on the initial conditions and as such it provides a very unique signature of an RS emission.

Swift<sup>(1)</sup> is expected to provide detailed optical observation of the early afterglow. In some cases the observation is expected to start before  $t_0$  and thus opens a unique window into the properties of the ejecta (in case that the ejecta is baryonic). Moreover, here we show that, if the prompt emission results from internal shock, then the light curve of the early optical afterglow at  $t < t_0$  is expected to be correlated with the prompt  $\gamma$ -ray emission (see fig. 1).

## 2. – The light curve at $t > t_0$ — a test of the reverse shock

After the reverse shock crosses the ejecta the shocked plasma cools and expand at the tail of the shocked external medium. Kobayashi and Sari [3] explored this phase numerically and they have shown that the evolution of the hydrodynamical parameters in the cooling ejecta depends weakly on the strength of the reverse shock (that in turn depends on the initial conditions of the ejecta). As a result the light curve during this phase depends on the initial condition only by the relative values of the three reverse shock break frequencies at  $t_0$  ( $\nu_a^r$ , the self-absorption frequency,  $\nu_m^r$ , the synchrotron frequency and  $\nu_c^r$  the cooling frequency). Over a wide range of the parameter space (assuming an ISM<sup>(2)</sup>) these frequencies satisfy  $\nu_{\text{radio}} < \nu_m^r(t_0) < \nu_a^r(t_0) < \nu_{\text{opt}} < \nu_c^r(t_0)$ , where  $\nu_{\text{radio}}$  and  $\nu_{\text{opt}}$  are the observed radio and optical frequencies, respectively [1]. In this case the optical light curve decays at  $t > t_0$  as  $\sim t^{-2}$  [4]. In contrast to the optical emission, the radio continues to rise at  $t > t_0$  and it peaks at a later time,  $t_*$ , when  $\nu_{\text{radio}} = \nu_a^r$ . Over a wide range of initial conditions (when the shock is not ultra relativistic)  $\nu_{\text{radio}} < \nu_m^r(t_0) < \nu_a^r(t_0) \approx 10^{12-13}$  Hz. In this case the radio emission is expected to rise first as  $\sim t^{0.5}$  until  $\nu_{\text{radio}} = \nu_m^r$  and then as  $\sim t^{1.25}$  until  $t_*$ . At  $t > t_*$  it is expected to decay, similarly to the optical emission, as  $\sim t^{-2}$ . This behavior implies that

$$(1) \quad \frac{F_*}{F_0} \left( \frac{t_*}{t_0} \right)^{(p-1)/2+1.3} = C \left( \frac{\nu_{\text{opt}}}{\nu_{\text{radio}}} \right)^{(p-1)/2} \sim 1000,$$

where  $F_0[F_*]$  is the peak optical [radio] flux (at  $t_0[t_*]$ ).  $C$  is a factor of the order unity that arises due to uncertainty in the hydrodynamics [3]. This entire evolution provides several independent tests to verify that we observe a reverse shock emission. It provides also an independent measurement of  $\nu_a^r(t_0)$ :

$$(2) \quad \nu_a^r(t_0) \approx \frac{t_*}{t_0} \nu_{\text{radio}}.$$

Detailed radio observations at  $t < t_*$  that identify the break during the rising phase, when  $\nu_m^r = \nu_{\text{radio}}$  would enable a determination of  $\nu_m^r(t_0)$  as well.

## 3. – Internal shocks and the reverse shock light curve at $t < t_0$

The reverse shock emission during the time that the shock crosses the ejecta depends strongly on the strength of the shock, and in particular on the value of  $n_0 \Gamma^2 / n_{\text{ejecta}}$

---

<sup>(1)</sup> <http://swift.gsfc.nasa.gov/docs/swift/swiftsc.html>

<sup>(2)</sup> If the external medium is a typical wind from a massive star then the density is much higher and as a result  $\nu_c^r(t_0) < \nu_{\text{opt}}$ . In this case the light curve evolution at  $t > t_0$  is different.

where  $n_0$  is the density of the ISM and  $\Gamma [n_{\text{ejecta}}]$  is the Lorentz factor [density] of the ejecta. The density profile of the ejecta before the internal shocks is not smoothed by the shocks, on the contrary, a density contact discontinuity is produced whenever an internal shock occurs within the ejecta. Therefore at the end of the internal shocks the density profile of the ejecta reflects the initial shells that produced the internal shocks. Since the *instantaneous* emission of the RS depends strongly on the density of the ejecta it would vary strongly whenever the RS crosses a density discontinuity that remains from the internal shocks. As a result of the angular smoothing [5, 6] the *observed* RS emission is an average of the *instantaneous* emission over a range of radii. This smoothing limits the variability time scale of the RS to be of the order of the observed time since the beginning of the prompt emission. Therefore, if the prompt  $\gamma$ -ray emission results from internal shocks, the RS optical light curve at  $t < t_0$  is expected to resemble a smooth version of the prompt  $\gamma$ -ray emission.

In order to demonstrate this relation between the prompt  $\gamma$ -ray emission and the reverse shock light curve at  $t < t_0$ , we have carried out a one-dimensional hydrodynamic numerical simulation<sup>(3)</sup>, starting before the internal shocks and ending long after the reverse shock crosses the ejecta. The initial conditions are four shells with Lorentz factors that vary between 60 and 240 with constant energy (see the inset in the top panel of fig. 1). The shells collide at a radius of  $\sim 2 \times 10^{14}$  cm and produce a prompt  $\gamma$ -ray emission composed of two pulses with a duration of approximately a second each. An illustration of the prompt  $\gamma$ -ray emission is depicted in the upper panel of fig. 1. Having the hydrodynamic evolution of the ejecta and the external medium we used a detailed synchrotron radiation code<sup>(4)</sup> to calculate the RS emission. The resulting optical light curve is depicted in the bottom panel of fig 1. The similarity between the two light curves is clear. Note also that in this specific case the optical reverse shock emission peaks long after the prompt  $\gamma$ -ray emission ends. This delay is expected when the ejecta is thin. In this case the ejecta expands linearly with the radius between the internal shocks radius ( $\sim 10^{14}$  cm) and the external shock radius ( $\sim 10^{16}$  cm). Figure 1 shows also that after the reverse shock crosses the ejecta,  $t > t_0$  the optical light curve is insensitive to the complex initial profile of the ejecta and it decays as  $t^{-2.1}$ .

\* \* \*

We thank R. SARI and S. KOBAYASHI for providing us with their relativistic hydrodynamics code and J. GRANOT, R. MOCHKOVITCH, F. DAIGNE and E. ROSSI for helpful discussions.

#### REFERENCES

- [1] NAKAR E. and PIRAN T., *MNRAS*, **353** (2004) 647.
- [2] SARI R. and PIRAN T., *ApJ*, **455** (1995) L143.
- [3] KOBAYASHI S. and SARI R., *ApJ*, **542** (2000) 819.
- [4] SARI R. and PIRAN T., *ApJ*, **520** (1999) 641.
- [5] FENIMORE E. E., MADRAS C. D. and NAYAKSHIN S., *ApJ*, **473** (1996) 998.
- [6] SARI R. and PIRAN T., *ApJ*, **485** (1997) 270.
- [7] NAKAR E. and GRANOT J., in preparation (2005).

---

<sup>(3)</sup> The hydrodynamics simulations were done using a one-dimensional Lagrangian code that was provided to us generously by Re'em Sari and Shiho Kobayashi [3].

<sup>(4)</sup> The synchrotron radiation code is described in [7].